Contents lists available at ScienceDirect

Chemical Engineering Research and Design

journal homepage: www.elsevier.com/locate/cherd

Application of high-frequency impedancemetry approach in measuring the deposition velocities of biomass and sand slurry flows in pipelines

Mahdi Vaezi[a,b], *Shubham Verma*[c], *Amit Kumar*[a,*]

[a] *Department of Mechanical Engineering, University of Alberta, Edmonton, AB, Canada*
[b] *Department of Technology, Northern Illinois University, Dekalb, IL, USA*
[c] *Department of Mechanical Engineering, Indian Institute of Technology, Kharagpur, India*

ARTICLE INFO

Article history:
Received 21 June 2018
Received in revised form 27 September 2018
Accepted 10 October 2018
Available online 17 October 2018

Keywords:
Biomass slurry
Sand slurry
Pipeline flow
Deposition velocity
Impedancemetry

ABSTRACT

Since the lower limit to operating velocities in slurry transport systems is influenced by deposition conditions, measuring the "deposition velocity" is an essential step in slurry pipelines' design and operation. This study proposes a new experimental technique in measuring deposition velocities in slurry pipeline transport called the high-frequency impedancemetry approach. This non-invasive technique of measuring electrical properties of substances, based on their frequency-dependent behavior, was applied using a 16-electrode impedancemetry device on a 25 m long closed-circuit pipeline to measure the deposition velocities of sand- and biomass–water mixture flows. Slurries of play and gravel sands, as well as wheat straw and wood chips biomass feedstock, were prepared over a range of concentrations (1.5–20 wt% dry-matter), and deposition velocities were measured over a wide range of operating velocities (0.04–4.5 m/s). Experimental measurements for sand–water mixtures were found to be in good agreement with empirical correlations derived previously through various analytical and mathematical techniques. In addition, for the first time, the deposition velocities for biomass–water mixtures were measured and found to be in the range of 0.21–0.8 m/s; surprisingly well below the common range of commercial pipelines' operating velocities, i.e., 1.4–3.0 m/s.

1. Introduction

Slurry (solid–liquid mixture) pipeline transport is a commercially viable mode of delivering solid commodities as an alternate to truck and rail. Since the 1960s, several commercial slurry pipelines have been constructed to hydraulically transport a variety of solids including coal (Abulnaga, 2002; Coffey and Partridge, 1982; Lahiri, 2009), limestone (Abulnaga, 2002; Venton, 1982), iron ore (Mariano De Souza et al., 2004), phosphate concentrate (Abulnaga, 2002; Weston and Worthen, 1987), and bitumen (Winter et al., 2003). However, slurry pipeline transport is a complex process that, as noted by Nardi (1959), to successfully design a pipeline to hydrotransport solids, designers need to consider as many as 32 variables (including 8 physical characteristics of the solid, 10 physical characteristics of the slurry, and 14 factors in design data) all at the same time. Predicting the prevailing flow regime and the longitudinal friction loss, as well as estimating deposition velocity, are the main technical issues to be addressed before constructing a slurry pipeline (Turian et al., 1987). The deposition velocity, also referred to as "the minimum carrying velocity" and "the limiting deposit velocity," is the lower limit to operating velocities for slurry transport systems with settling (heterogeneous) slurries containing particles predominantly larger than 50–70 μm (Grzina et al., 2009). Deposition velocity is commonly defined as "the minimum velocity demarcating flows in which the solids form a bed at the bottom of the pipe from fully suspended flows" (Oroskar and Turian, 1980).

There have been several analytical correlations proposed to predict the deposition velocity for slurry transport in pipelines. After conducting a series of experiments, Durand (1953) and Durand and Condolios

* *Corresponding author.*
E-mail address: amit.kumar@ualberta.ca (A. Kumar).
https://doi.org/10.1016/j.cherd.2018.10.013

Nomenclature

C_D	Drag coefficient for free-falling sphere
C_m	Concentration, mass fraction, wt%
C_V	Concentration, volume fraction, vol%
d	Particle diameter, m
D	Pipe diameter, m
$\bar{D}$	Absolute average percent deviation
d_{50}	Corresponding particle lengths in mm at respective 50% cumulative number fractions of particles
D_v	Percent deviation
EGS	Environmental gravel sand
ERT	Electrical resistivity tomography
f(C_V,s)	Function of particle concentration
g	Gravitational acceleration, m/s^2
ID	Internal diameter
k, I, m	Constants
MC	Moisture content
μ	Fluid viscosity, kg/m.s
N	Number of data points
ρ	Density of liquid, kg/m^3
ρ_s	Density of solid, kg/m^3
R	Impedance across the impedancemetry device
R_o	Series resistance (5 kΩ)
RMS	Percent root mean square variation
s	ρ_s/ρ, Solid to liquid density ratio
v	Slurry velocity, m/s
v_c	Deposition velocity, m/s
V_m	Voltage across the impedancemetry device
V_F	Output voltage from the function generator

(1952) were among the first to propose a correlation to define limiting deposit velocity. Wasp et al. (1977) extended their correlation to correct for solid concentrations and account for a wider range of particle diameters. Oroskar and Turian (1980) proposed a theoretical model based on turbulence theory that considered the deposition velocity to be the point where all the solid particles are in suspension by the vortices caused by turbulence. However, there have always been wide discrepancies in the predictions by various correlations. Turian et al. (1987) reviewed 31 correlations (including the ones discussed above), recast them all into a standard form, and compared with a large collection (864 data points) of published, experimentally measured, deposition velocity data. It is obvious on comparing the expressions shown in Table 1 that qualitative disparities among the seven correlations studied here are quite broad; a deviation of 26–50% was observed. For the 31 correlations listed by Turian et al. (1987), however, the deviations range from 25 to 750%, with an average of 92%.

Although the deposition condition is difficult to discern, the slurry flow appears unstable near it, and the deposition velocity is difficult to determine experimentally, the concerns associated with the uncertainty of theoretical and empirical correlations have allowed the experimental techniques to remain viable options in the measurement of slurry flows' deposition velocities.

Although visual observation through a section of transparent pipe is still applied to measure deposition velocities whenever possible, high fines concentrations (that limit visibility) and large pipes make it challenging in practice and thus it is necessary to use another method. Gillies et al. (2000) and Gillies and Shook (1991) used a gamma ray densitometer beam to span the pipe on a horizontal chord close to the bottom and measured the mean concentration of the solids vs. changing bulk velocity. With decreasing bulk velocity, the chord concentration increased slowly at first and rapidly later, right when deposition occurred. Shah and Lord (1991) used a differential pressure transducer together with a magnetic flow meter to gather steady-state differential pressure vs. flow rate (velocity) data at decreasing slurry flow rates over a wide range of slurry concentrations. Differential pressure and flow rate data were then represented in terms of logarithmic plots of wall shear stress vs. nominal shear rate where deposition velocities corresponding to minimum wall shear stress were determined.

Table 1 – Comparison of published deposition velocity correlations in slurry transport.

Standard form of correlations

$$\frac{v_C}{\left[2gD(s-1)^{0.5}\right]} = f(C_V, s)\, C_D^k \left[\frac{D\rho[gD(s-1)]^{0.5}}{\mu}\right]^l \left(\frac{d}{D}\right)^m$$

No.	Authors	f(C,s)	k[c]	l	m	$\bar{D}$[a]; RMS[b]
1	Durand and Condolios (1952)	1.153 (C_V = 0.0197) 1.307(C_v = 0.04) 1.326(C_v = 0.0628) 1.423(C_v = 0.0864)	0	0	0	36.53; 0.4074 for $f(C,s)$ = 1.2
2	Wasp et al. (1977)	$3.399C_V^{0.2156}$	0	0	1/6	26.68; 0.3750
3	Knoroz (reported by Sasic and Marjanovic, 1978)	$0.8165\left[\frac{sC_V}{1-C_V}\right]^{1/6}$	−0.5	0	−1/12	51.01; 0.6695
4	Zandi and Govatos (1967)	$(20C_V)^{1/2}$	−1/4	0	0	50.02; 0.6521
5	Larsen (1968)	$2.9818C_V^{1/4}$	−1/4	0	0	45.22; 0.6090
6	Shook (1969)	$2.43C_V^{\frac{1}{3}}$	−0.25	0	0	34.50; 0.5059
7	Oroskar and Turian (1980)	$1.414\left[5C_V(1-C_V)^{2n-1}\right]^{8/15}$	0	1/15	0	25.94; 0.4331 For n = 2

[a] $D_V\,(\%dev) = \left[\frac{v_{C(calc)} - v_{C(exp)}}{v_{C(exp)}}\right] \times 100$ and $\bar{D} \equiv Abs.avg.\%dev. = \sum_{i=1}^{N} \frac{|D_{Vi}|}{N}$.

[b] $RMS \equiv \left\{\sum \frac{\left[v_{C(calc)} - v_{C(exp)}\right]^2}{N}\right\}^{0.5}$.

[c] All k, l and m coefficients are adopted from Durand and Condolios (1952) reported by Oroskar and Turian (1980).

Table 2 – Properties of various sand and biomass particles and their corresponding water-based slurries.

Particle	Type	Mass median particle diameter – d_{50} (mm)[a]	Particle density (kg/m^3)	Slurry concentration (wt% – saturated)[b,c]	Slurry concentration (wt% – dry)[c]	Slurry concentration (vol% – dry)[c]
Sand	Play sand	0.445	2650	NA	5	1.9–8.6
	Environmental gravel sand	0.630			–20	
Agricultural residue	Fine wheat straw	4.81	1250	10–30	2–6.5	2–6.3
	Large wheat straw	9.7		10–20	2–4.2	2–4.1
Forest residue	Fine chips (aspen and poplar)	1.91	1450	10–40	3–13	2.2–9.6
	Large chips (spruce and pine)	7.18		5–10	1.5–3	1–2.2

[a] Corresponding particle lengths in mm at respective 50% cumulative number fraction of particles.
[b] With 82% saturated moisture content for agricultural residue and 70% for forest residue particles.
[c] Maximum concentration tested was limited by the pipeline diameter and the pumping capacity.

Following the electrical resistance tomographic (ERT) approach (see, for instance, (Dickin and Wang, 1996)), Fangary et al. (1998) used a 16-electrode sensor system with a current injection amplitude of 5 mA at a frequency of 10 kHz together with a back-projection image reconstruction algorithm to monitor the thickness of solids deposited on the base of a horizontal pipe. Fangary managed to detect the transition from a dispersed to a salting suspension. The latter produced a detectable perturbation on the reconstructed conductivity map at the bottom of the pipe cross section due to a change in the mean solid concentration in the flowing bulk suspension that was distinct from that in the settling region.

All four experimental approaches discussed above, although effective, come with inadequacies: Gillies and Shook (1991) reported ~10% error in visual observations compared to densitometer measurements. With gamma ray densitometry, a compromise must be made between accuracy and applicability. The larger aperture brings about higher intensity/accuracy but limits the measurement to the parts with sufficiently large test areas of constant thickness. In addition, safety requirements/regulations to install/operate gamma ray densitometry are restrictive (Schlieper, 2000). With pressure transducers, if the flush diaphragm type is not used, it is challenging to prevent solid particles from disturbing/stopping measurements. Furthermore, at lower slurry flow rates, friction losses are too small to be accurately detected by typical transducers (Vaezi et al., 2014a). Finally, the ERT (electrical resistivity tomography) system is sophisticated (comprised of sensors, sinewave generator, multiplexer, digital de-modulation, etc.) and costly, and data collection strategies and image reconstruction algorithms are difficult to apply. In addition, the ERT approach, to be applicable, requires a significant electrical conductivity difference between solid particles and fluid (Yenjaichon et al., 2011).

The high-frequency impedancemetry approach is a non-invasive technique of measuring electrical properties of substances based on their frequency-dependent behavior. Although it has been widely used in biology and biotechnology (Dezenclos et al., 1994; Dheilly et al., 2008), as well as in a variety of clinical applications from hematology (Brahimi et al., 2010) to nephrology (Caillette et al., 1994; Smye et al., 1994) to nutrition (Bott, 2006; Ellis et al., 2000), the aim here was to develop and validate a methodology to apply high-frequency impedancemetry in the pipeline transport of solid commodities to measure the slurry flows' deposition velocities. Accordingly, a 16-electrode impedancemetry device was designed, fabricated, and installed on a 25 m long and 50 mm in diameter closed-loop pipeline facility to measure the deposition velocity of sand–water mixtures, as well as biomass–water mixture flows. Unlike previous deposition velocity measurement techniques, the device proposed here does not disturb/stop the slurry flow and is simple and economical to fabricate (a minimum of two conductive electrodes on a non-conductive piece of pipe are needed), easy to operate (no programing or post-analysis required), easy to mount on the pipeline (could be flanged anywhere along the pipeline), applicable to all the suspensions conducting electricity, and capable of accurately measuring slurry deposition velocities as low as 0.04 m/s. In light of all of these features, the high-frequency impedancemetry approach can become the standard deposition velocity measurement technique. Following are the specific objectives of the present research study:

- Proposing application of high-frequency impedancemetry technique in experimentally measuring deposition velocities of slurry (i.e., solid–liquid mixture) flows in pipes,
- Designing, fabricating, installing, and calibrating a 16-electrode impedancemetry device on a lab-scale closed-circuit pipeline facility,
- Proving the viability of the proposed high-frequency impedancemetry approach in measuring the deposition velocities of slurry flows in pipes in a simple, fast, and accurate manner, and
- Measuring the deposition velocities of forest- and agricultural residue-water mixture flows in pipeline hydro-transport of biomass feedstock for biofuel production purposes.

2. Methodology

2.1. *Commercial pipeline operating velocity*

The commercial operating velocity for pipelines has been reported differently for various commodities. To prevent erosion by solids, noise, or water hammer caused by quickly closing a valve, pipeline operating velocities must not exceed a maximum, nor should they drop below a minimum in order to keep the line swept clear of entrained solids and liquids. The maximum and minimum velocities are normally set to 4.5 m/s and 0.9 m/s, respectively (Abulnaga, 2002). However, the acceptable range commonly practiced in industry is 1.4–3.0 m/s (Leitch, 2006). Operating (i.e., slurry) velocities experimented within this study range from 0.04 to 4.5 m/s, which covers well the range used in commercial applications for all sorts of commodities (oil sands, iron ore, coal, etc.) reported in earlier studies (Coffey and Partridge, 1982; Venton, 1982; Mariano De Souza et al., 2004; Winter et al., 2003). It is worth mentioning that investigating other velocity-dependent phenomena such as erosion is out of the scope of the present research.

2.2. *Experimental setup and slurry preparation*

Three types of particles — sand, agricultural residue biomass (i.e., wheat straw), and forest residue biomass (i.e., wood chips) — were tested. The solid particles were chosen purposely since (1) pumping sand–liquid mixtures is commonly practiced in the oil sands and dredging industries (Matousek, 2001, 2002), (2) there exist a large body of experimental data previously pyblished on sand–water mixture flows which will be used for comparison/validating purposes, (3) the bioenergy sector is investigating the technical and economic feasibility

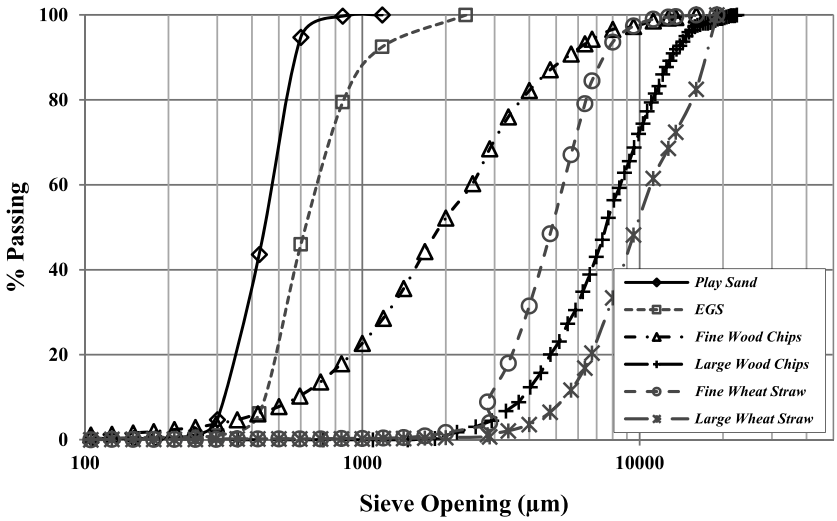

Fig. 1 – Size distribution of sand, agricultural residue, and forest residue particles.

of pipelining forest- and agricultural residue-water mixtures to bio-based energy facilities for the large-scale production of bio-fuels (Vaezi et al., 2013; Vaezi et al., 2014a; Vaezi, 2014b; Vaezi and Kumar, 2014; Vaezi et al., 2015). Play sand as well as environmental gravel sand (EGS) were supplied by Sil Industrial Minerals, wheat straw was collected from a farm in northern Alberta, Canada and Weyerhaeuser Pembina Timberlands Company provided large (spruce and pine) and small (aspen and poplar) wood chips. Table 2 gives the specifications of the particles. Size distributions of the particles are shown in Fig. 1.

A schematic illustration of the experimental setup is provided in Fig. 2. The setup is comprised of 25 m long, 50 mm ID, schedule 40 steel pipe with a clear acrylic section, long and short radius bends, and horizontal, inclined, and vertical orientations. The liquid (water) and solid particles were mixed to the desired concentration (see Table 2) in a vessel equipped with a 0.37 kW centrally placed mixer (EV6P50M; Lightning Inc., Rochester, NY, USA) with a double, three-bladed impeller. The slurry flow was provided by a specifically designed 7.45 kW centrifugal pump (CD80M; Godwin Pumps Ltd., Bridgeport, NJ, US) coupled with a 7.45 kW induction electric motor (CC 068A; Madison Industrial Equipment, Vancouver, BC, Canada) and controlled by a 14.9 kW variable frequency drive (VFD) controller (MA7200-2020-N1, TECO-Westinghouse Co.). Slurry temperature was monitored and adjusted to maintain an approximately isothermal condition (about 15 °C) using a double-tube heat exchanger. The setup was also equipped with an electromagnetic flow meter (FMG-401H; Omega Eng., Stamford, CT, USA), a resistance temperature detector (RTD-E; Omega Eng., Stamford, CT, USA), flush diaphragm low-pressure transmitters (PX42G7; Omega Eng., Stamford, CT, USA), and a watt transducer (PC5; Flex-Core, Columbus, OH, USA). The output signals from the equipment were recorded on a one-hundred-data-per-second basis on a data acquisition system comprised of a 4-channel current excitation module (NI 9219; National Instrument Corp., Austin, TX, USA) and a data acquisition program (LabView V.9.0.1f2; National Instrument Corp., Austin, TX, USA).

Solid–liquid mixtures were prepared over a range of particle types (sand, agricultural residue, forest residue), particle dimensions (d_{50} from 0.4 to 9.7 mm), and slurry concentrations (from 1.5 to 20 wt% dry matter).[1] Table 2 presents the range of the slurry concentrations restricted by mechanical constraints, e.g., pump power and pipe diameter. Forest and agricultural residue biomass slurries were circulated at high flow rates (4.5 m/s) for 8–12 h before stable mixture properties (the particle's moisture content [MC] and dimensions, carrier liquid density and viscosity, mixture air content) and operating conditions (pressure and velocity fluctuations less than 1% per hour) were attained (Vaezi and Kumar, 2014). Measurements were then made on a slurry of a known particle type and size while the flow rate was decreased from 4.5 to 0.04 m/s using a variable frequency drive (VFD) controller and on the slurry concentration by adding clear water to the mixing vessel.

2.3. *High-frequency impedancemetry approach*

An impedancemetry device was designed and fabricated and mounted on one horizontal section of the pipeline setup (Fig. 2 — Section 4). The device is comprised of 16 electrodes (stainless steel cylinders 2.95 mm in diameter) with a wide base (20 mm long, 6 mm wide, 3 mm in depth) precisely inserted through the wall of a non-conductive plastic pipe (52.5 mm in diameter) to lie along the inner wall so as not to disrupt the slurry flow in any way (Fig. 3). On the sides of the measurement device, a non-reactive non-conductive plastic collar and a stainless steel tightener are used to ensure a tight seal between the collar and the measurement device. This device has flanges at each end to facilitate mounting and dismounting when/where needed (Fig. 3(d)).

"Electrical impedance", or simply impedance, describes a measure of opposition to alternating current (AC); it extends the concept of resistance to AC circuits, describing not only the relative amplitudes of the voltage and current, but also the relative phases. The slurry, together with the impedancemetry device, formed a resistive-capacitive circuit with a capacitance independent of the slurry concentration. Since the capacitive reactance (impedance of the capacitor) is inversely proportional to the frequency of the applied voltage, a high-frequency voltage was applied here in order to cancel the capacitive effect (the reac-

[1] On unit weight basis of dry-matte (0% moisture content) solid mass contents.

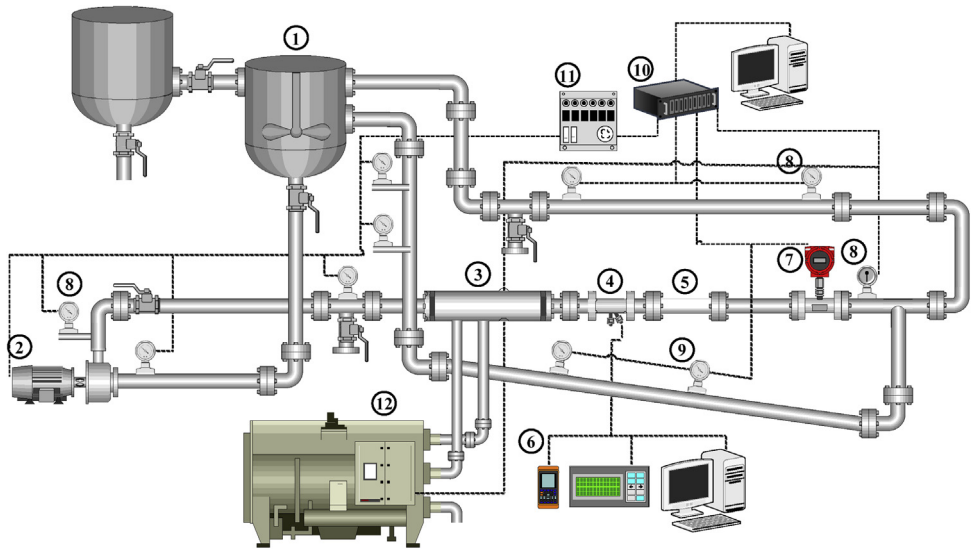

Fig. 2 – Pipeline facility in the Large Scale Fluids Lab. (1) mixing tank, (2) centrifugal slurry pump, (3) heat exchanger, (5) clear acrylic section, (4) impedancemetry device, (6) impedance measurement system (7) magnetic flow meter, (8) temperature sensor, (9) pressure transducer, (10) data logger, (11) watt transducer, (12) cooling unit.

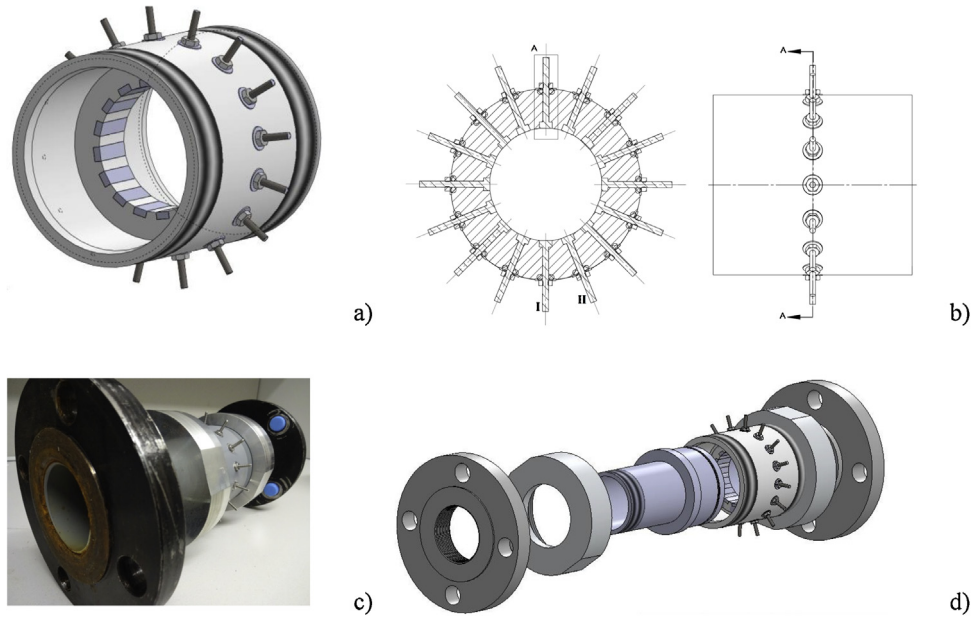

Fig. 3 – (a) Schematic of the impedancemetry device with 16 electrodes, (b) side and cross sectional view of the impedancemetry device with 16 electrodes including the two adjacent electrodes (I & II) across which the impedance was measured, (c) electrical impedance measurement section fabricated in the Large Scale Fluids Lab, (d) Assembly of the measurement section including impedancemetry device, collars, tighteners, and flanges.

tance of the capacitor would be no longer dominant); hence the name of the approach high-frequency impedancemetry.

Fig. 4 gives a schematic of the impedance measurement system. The input voltage, a sinusoidal wave with an RMS voltage amplitude of 10 V at 100 kHz frequency, was provided through a function generator (GFG-8216A, GwInstek, Good Will Instrument Co., New Taipei City, Taiwan). Since the greatest impedance measured throughout the experiment was 8 kΩ, a 5 kΩ (nearly half the maximum impedance) resistance was used through the circuit to reduce the noise. The voltage across the impedancemetry device (the two electrodes) was measured using a true RMS multimeter (U1242A, Agilent, Santa Clara, CA, USA). The use of a true RMS multimeter rather than a AC rectified average multimeter was necessary to accurately measure the impedancemetry output AC voltage since the slurry, when excited with a sinusoidal wave, generated an impure sinusoidal output wave. The voltage measured across the electrodes was then converted into impedance by using the correlation below:

$$R = V_m R_o / (V_F - V_m) \quad (1)$$

The impedance was measured across two adjacent electrodes (I and II — Fig. 3b) of the impedancemetry device. Measuring impedance along adjacent electrodes was found to give the least noise and fluctuations. Moreover, electrode I is the first one that comes in contact with the settling solid particles. Therefore, electrode I should necessarily be one of the two electrodes across which the impedance is measured.

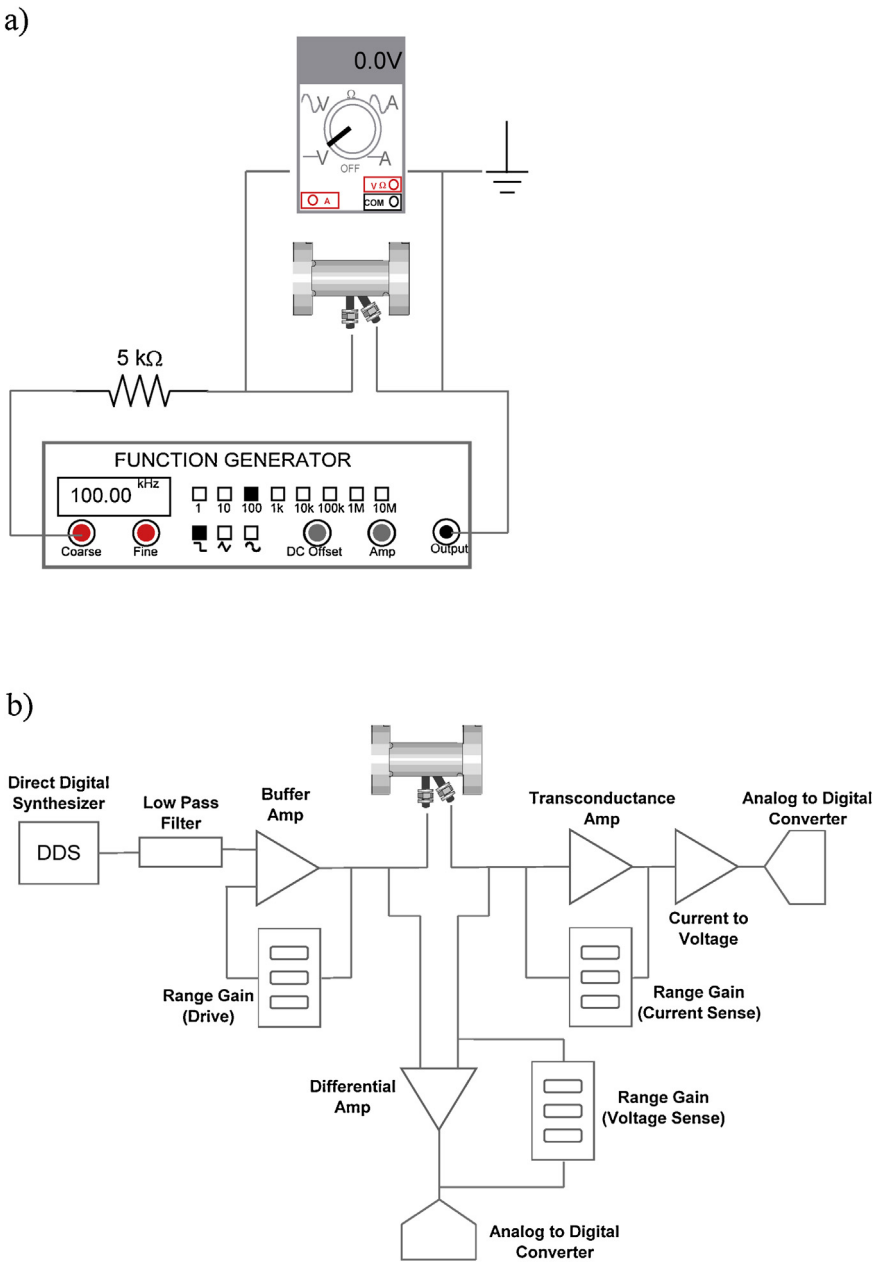

Fig. 4 – (a) Impedancemetry setup circuit diagram, (b) LCR meter circuit diagram.

Electrical connections were made from the dry side of the electrodes and then impedance was measured using the impedancemetry device along with (1) the impedancemetry setup circuit (Fig. 4a) and (2) the LCR meter (an electronic test equipment used to measure the inductance (L), capacitance (C), and resistance (R) — Fig. 4b). The programmable automatic LCR meter used here (PM 6304, Fluke Corp., Mississauga, ON, Canada) is an electronic device that measures the inductance (L), capacitance (C), and resistance (R) of a component (the meter measures the AC voltage across, and the current through, the device under test and the corresponding ratio determines the magnitude of the impedance). The impedance was measured using the LCR meter as well in order to validate the accuracy and reliability of the impedancemetry setup circuit. While the impedancemetry setup circuit proposed here is comprised of pieces easily found in most electrical labs and can be quickly and economically assembled, the LCR meter is an expensive piece of high-precision instrument. It is also important to note that the magnitude of the impedance measured by both methods was different. This is because of the internal resistance of the individual devices in the circuit, as well as the differences in their measurement techniques.

2.4. *Impedance measurement procedure*

First, clear water was circulated throughout the experimental setup to measure the lower range of the impedance along electrodes I and II on the impedancemetry device. It was observed that the impedance of the circuit (Fig. 4a) changed with time (see Fig. 5a). Although the change in impedance was negligible, clear water was circulated in the loop before solid particles were added until a stable value of impedance was achieved. Initial built-up rust in the pipe was the main reason behind the variation of water impedance. Premeasured magnitudes of solids were then added to achieve favorite slurry concentration (see Table 2) while the slurry circulated at the maximum achievable flow rate to prevent settling along the pipeline bottom. Once stable mixture properties and operating conditions were attained (see Section 2.1), impedance and

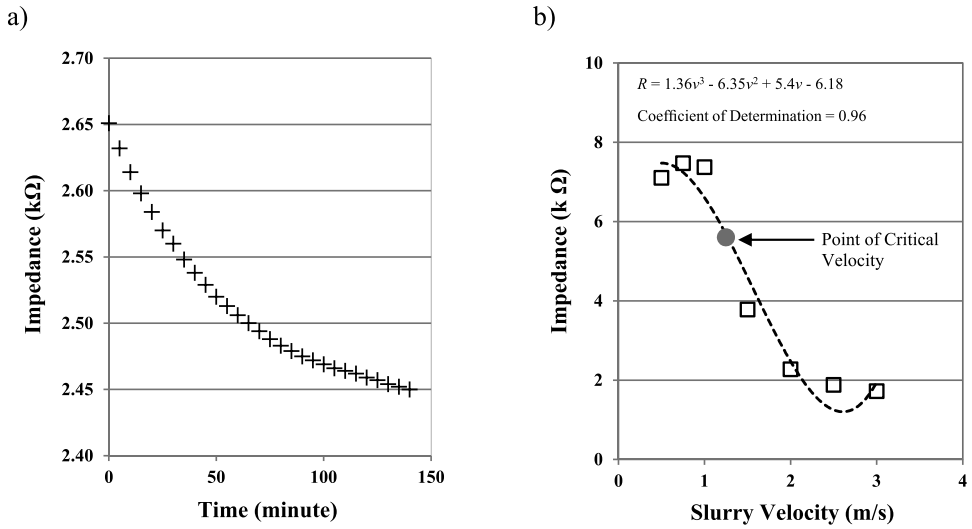

Fig. 5 – (a) Impedance vs. time for circulating clear water in the pipeline setup, (b) general trend of the impedance vs. velocity graphs with the schematic point of deposition velocity.

flow rate data were gathered using both the impedancemetry setup circuit and the LCR meter while the flow rate was gradually decreased from 4.5 to 0.04 m/s (the decrease in flow rate was made in steps of 0.5 m/s when there was no sign of solid deposition and in steps of 0.1 m/s when the formation of a moving bed was noticed). Deposition was observed visually as well in a section of transparent pipe (Fig. 2 — Section 5) whenever possible. Once the measurement of impedance at certain slurry concentration over the entire range of flow rates was complete, pumping velocity was increased back to the maximum of 4.5 m/s. While the slurry circulated at a high flow rate, either additional solid particles (in sand–water mixtures) or clear water (in biomass–water mixtures) was added to prepare the subsequent slurry concentration (although in practice solid particles are added to gradually increase the slurry concentration, in the case of biomass–water mixtures, because of the time it takes for the biomass solid particles to absorb water and become fully saturated, water was added to adjust/decrease the concentration). The entire experiment was then repeated the same way as described above. These steps were repeated until all solids concentrations were experimented with as per the ranges shown in Table 2.

The graphs in Fig. 5b show the general trends of impedance vs. velocity obtained through experimental measurements. The lower extreme represents fully suspended particles and the upper extreme corresponds to a stationary bed. The steep rise in the impedance is related to the formation of a moving bed. The same trend was reported by Gillies et al. (2000) and Gillies and Shook (1991) for variations in concentration along a horizontal chord close to the bottom of the pipe vs. pumping velocity.

The graphs were fitted to third order polynomial equations. The deposition velocity was then calculated at the point of inflection (by equating the second derivative of the polynomial function zero), implying a change in flow behavior from fully moving bed to part stationary bed with saltation, rolling, and ripple movement. Sample experimental measurements, corresponding third order polynomial trend lines and functions, and the point of inflection are marked on a schematic impedance-velocity graph on Fig. 5b.

3. Results and discussion

3.1. *Sand–water mixtures*

Fig. 6 shows the variation of the impedance vs. the slurry flow rate for 5 to 20 wt% play sand–water mixtures in the pipeline setup. By looking at the graphs, one can quickly make an engineering estimation of the deposition velocity around the point at which the concavity changes. A more accurate value was obtained by fitting a polynomial curve to the experimental points and calculating the point of inflection. The polynomials with the order of three were examined to find the appropriate curve that makes the best fit to the experimental measurements and comes with the highest coefficient of determination. To improve the overall fit of the estimated regression line, only the part of the line with a steep slope (corresponding to the formation of moving and stationary beds) was considered.

The applicability of the impedancemetry device, the accuracy of the impedancemetry setup, and the reliability of the high-frequency impedancemetry approach were investigated. Table 3 and Fig. 7a present the deposition velocities of sand–water mixtures containing coarse and fine particles measured using the impedancemetry device. A sharper increase in deposition velocity with increases in concentration is observed at lower concentrations for environmental gravel sand particles; i.e., 5–10 wt%. However, the range of concentrations tested for smaller play sand particles, was not wide enough to visually observe this effect. Adding more particles to the enclosed area of the pipe slows the slurry flow more than expected (hindered settling effect) and counteracts particle settling, which explains the smaller or reverse dependency of the deposition velocity on concentrations at higher concentrations. Turian et al. (1987) and Gillies et al. (2000) reported similar phenomena while investigating deposition velocities in pipeline flow of slurries. In terms of particle diameter, the deposition velocity has a rather weak dependence on particle diameter. The same conclusion has been

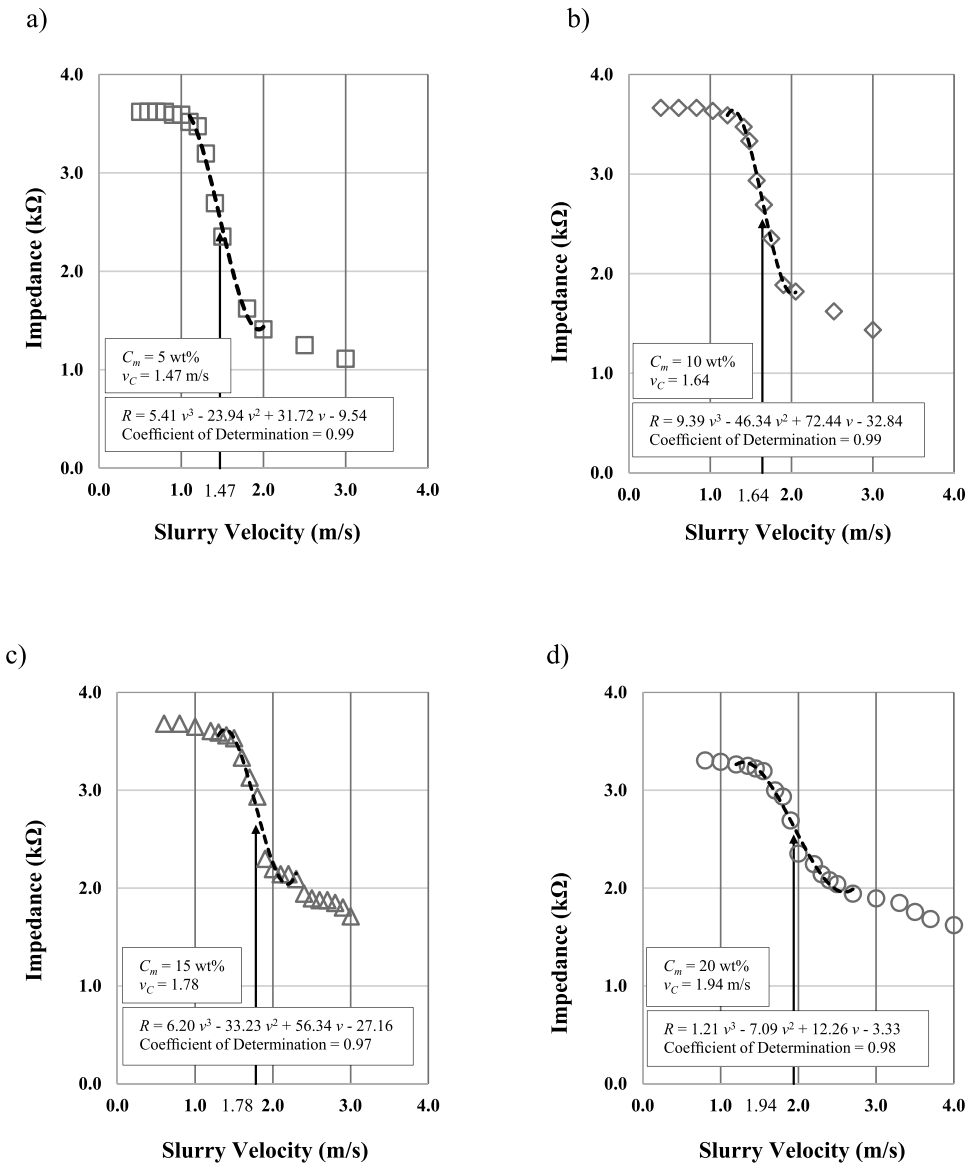

Fig. 6 – Impedance vs. slurry velocity for play sand–water mixtures over 5–20 wt% slurry concentrations measured using the impedancemetry device.

Table 3 – Deposition velocity for various concentrations of sand–water mixtures flows.

Particle type	Slurry concentration (C_m, wt%)	Deposition velocity (v_C, m/s)		Deviation[a] (D_V, %)
		Impedancemetry setup	LCR meter	
Play sand (fine)	20	1.94	1.87	3.7
	15	1.78	1.79	-0.5
	10	1.64	1.63	0.5
	5	1.47	1.39	5.2
Environmental gravel sand (coarse)	20	1.85		
	15	1.76		
	10	1.26		

[a] $D_V\,(\%dev) = \left[\frac{v_{C(impedancemetric)} - v_{C(LCR)}}{v_{C(impedancemetric)}}\right] \times 100.$

made by Turian et al. (1987), who suggest $v_C \sim d^{\circ}$ specially for large non-colloidal particles. This confirms the applicability of the impedancemetry device in measuring the deposition velocity of slurries of various particle diameters and concentrations.

To study the effect of temperature on deposition velocity, a play sand-water mixture was circulated through the pipeline at 28 °C and 42 °C. Impedance magnitudes were then recorded over a range of slurry velocities and corrected according to the change in temperature over time using a correlation proposed by Giguere et al. (2008), as follows:

$$R_{T,ref} = R_T[1 + \alpha\,(T - T_{ref})] \quad (2)$$

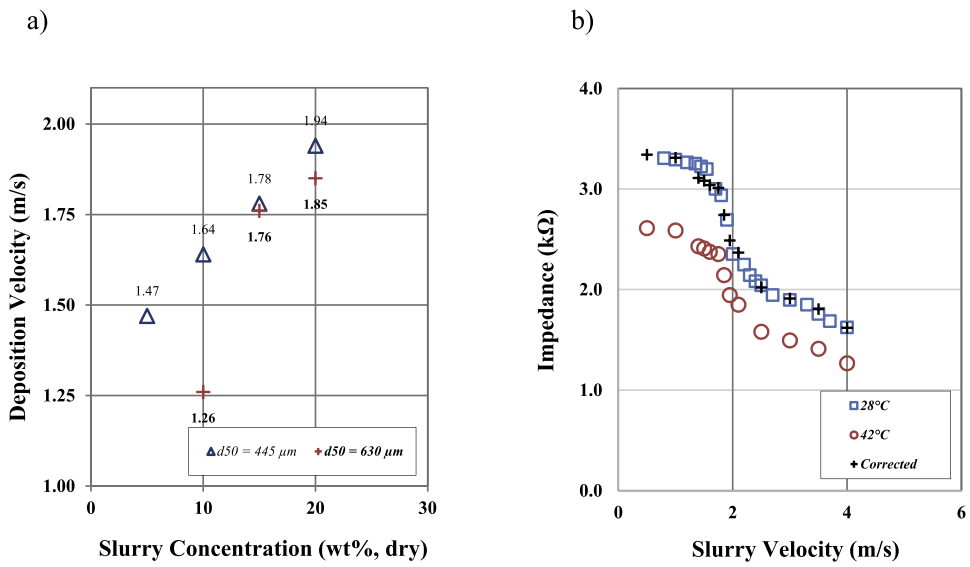

Fig. 7 – (a) Deposition velocity vs. slurry concentration for play sand- and gravel sand–water mixtures over a range of slurry concentrations, (b) impedance vs. slurry velocity for play sand–water mixtures at various temperatures.

where $R_{T,ref}$ is the resistance at reference temperature T_{ref}, R_T is the resistance at temperature T, and α is the thermal resistance coefficient ($\alpha = 0.02$ satisfies the equation in our experiment). It is observed on Fig. 7b that, after accounting for the change in impedance due to the change in temperature, the impedance values were almost identical in both slurry temperatures. This suggests that the change in impedance was merely caused by the change in slurry temperature and not any other change in the property of the liquid, e.g., viscosity of the carrier fluid. For consistency purposes, isothermal conditions (about 15 °C) were retained here throughout the whole experiment.

The experimental values obtained here for the deposition velocities of various concentrations of play sand–water mixtures using the impedancemetry setup was re-measured with the LCR meter as well. Fig. 8 and Table 3 compare the two measurements and corresponding deviations. For the same slurry concentration, although there is a noticeable difference in the magnitude of impedance measured by the two techniques (see Section 2.2), corresponding deposition velocities are in excellent agreement with an average deviation of 2.22% only, thus confirming the accuracy and reliability of the impedancemetry setup.

The experimental approach proposed here was compared with empirical correlations proposed in literature. The deposition velocities experimentally measured were theoretically predicted as well using experimental facility dimensions and slurry properties plugged into five of 31 correlations reviewed by Turian et al. (1987) originally proposed by Oroskar and Turian (1980), Shook (1969), Larsen (1968), Zandi and Govatos (1967), and Knoroz originally reported by Sasic and Marjanovic (1978) for gravel- and play sand–water mixtures. Corresponding empirical correlations are reported in Table 1. As observed on Fig. 9, the deposition velocities obtained using these correlations turned out to be in good agreement with the experimental measurements with deviations ranging from 6.2 to +33% and average deviations of −8.3% for play sand–water mixtures and 6.9% for gravel sand–water mixtures. This is well below the average 92% deviation between empirical correlations and 864 experimentally measured deposition velocity data points (see Table 1) reported by Turian et al. (1987). This, as well, proves the viability of the high-frequency impedancemetry approach in measuring the deposition velocities of solid–liquid mixtures in pipes in a simple, fast, and accurate manner.

It is worth mentioning that although a change in the diameter of the pipeline would change the deposition velocities obtained here, the effect of the pipe diameter was not particularly studied here. The present research is focused on introducing a new approach of experimentally measuring deposition velocities and, for that reason, only one pipe diameter of 50 mm has been considered for validation and comparison purposes.

3.2. *Agricultural and forest residues*

The same approach as for the sand–water mixtures was applied to measure the deposition velocities in agricultural and forest residue-water mixtures. Fig. 10 shows the experimental measurements using the impedancemetry device as well as the LCR meter for slurries of various diameters of wheat straw and wood chip particles over a wide range of concentrations (1.5–13 wt% dry matter). A good agreement was found between impedancemetry and LCR measurements; in addition, a trend line similar to the lines for sand–water mixtures was obtained in all case scenarios. Table 4 lists the deposition velocities for all the wheat straw- and wood chip-water mixtures experimented here. As it can be observed, the deposition velocities were relatively small, ranging from 0.21 to 0.8 m/s, and no meaningful relations were found between the slurry concentrations and the deposition velocities. The velocity ranges are well below the common range of operating velocities in industrial pipelines, i.e., 1.4–3.0 m/s (Abulnaga, 2002) (see Section 2.1). This, surprisingly, implies that while pumping biomass–water mixtures in pipelines under the conditions studied here (i.e., material type, particle size, slurry concentration, commercial velocity range), no deposition will be observed. This is good news for the pulp and paper and the biofuel sectors, which are actively exploring the option of replacing truck delivery of biomass feedstock by pipeline hydro-transport. Knowing that there are no deposition concerns considerably simplifies the design and operation of biomass slurry pipelines. To the best of the authors' knowledge, this is the first time this feature is observed and reported.

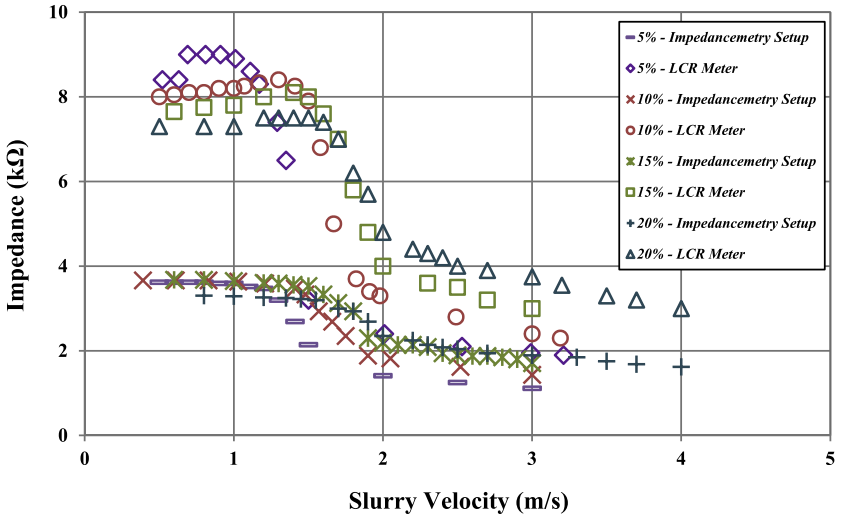

Fig. 8 – Impedance vs. slurry velocity for play sand–water mixtures of various concentrations measured using the impedancemetry circuit and the LCR meter.

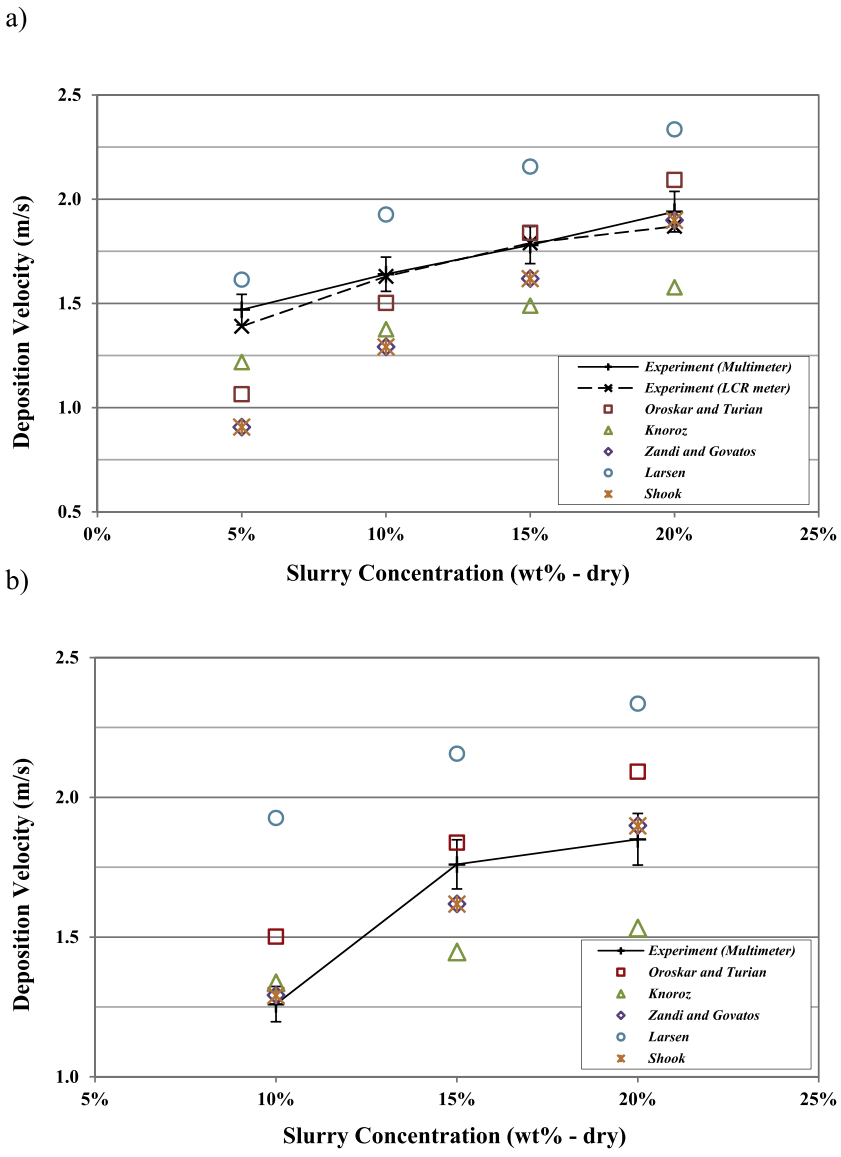

Fig. 9 – Experimental vs. numerical/empirical correlation results for the deposition velocities of (a) play sand–water mixtures and (b) gravel sand–water mixtures in pipes.

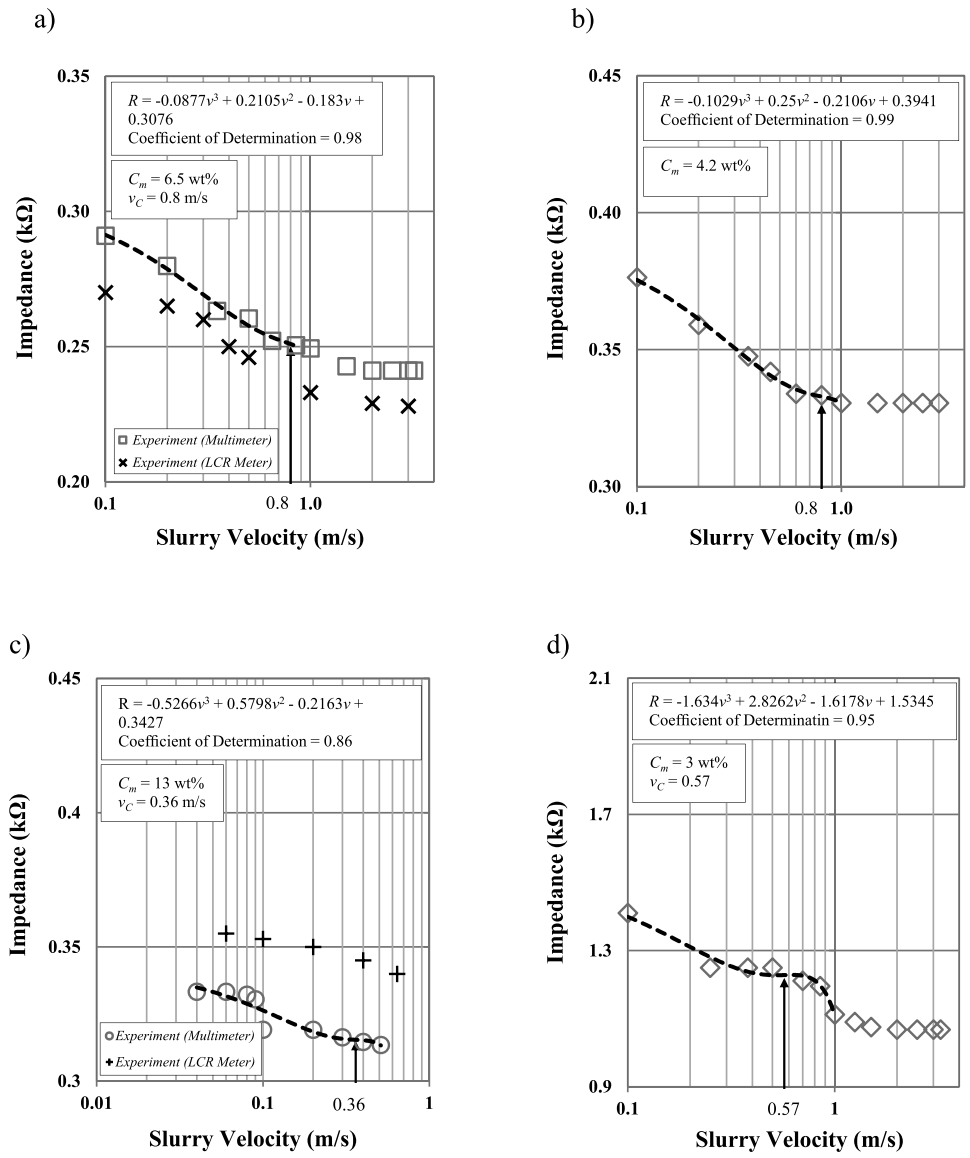

Fig. 10 – Impedance vs. slurry velocity for (a) 6.5 wt% dry-matter slurry of 4.8 mm wheat straw particles, (b) 4.2 wt% dry-matter slurry of 9.7 mm wheat straw particles, (c) 13.0 wt% dry-matter slurry of 1.9 mm wood chips particles, and (d) 3.0 wt% dry-matter slurry of 7.1 mm wood chips particles measured using the impedancemetry device.

Table 4 – Deposition velocity for various concentrations of biomass–water mixture flows measured using the impedancemetry setup.

Particle type	Particle size	Slurry concentration (C_m, wt% – dry)	Deposition velocity (v_C, m/s)
Wheat straw	Fine (d_{50} = 4.81 mm)	2.0	0.21
		4.2	0.28
		6.5	0.8
	Large (d_{50} = 9.7 mm)	2.0	NA
		3.1	0.8
		4.2	0.8
Wood chips	Fine (d_{50} = 1.91 mm)	3.0	0.44
		6.2	0.55
		9.5	NA
		13	0.36
	Large (d_{50} = 7.18 mm)	1.5	0.52
		3.0	0.57

4. Conclusion

The high-frequency impedancemetry technique was applied here for the first time to measure the slurry flow deposition velocity in pipeline transport of solids. A 16-electrode impedancemetry device was designed, fabricated, and installed on a 25 m long and 50 mm in diameter closed-loop pipeline facility to measure the deposition velocity of sand (play sand and environmental gravel sand)-water mixtures and biomass (wheat straw and wood chips) slurry flows.

Sand- and biomass–water mixtures were prepared over a wide range of concentrations (1.5–20 wt%, dry) and pumped over a range of velocities (0.04–4.5 m/s) much wider than the common industrial practice of 1.4–3.0 m/s. Besides the impedancemetry device, the LCR meter was used to measure the slurry flow deposition velocity to validate accuracy and reliability of the impedancemetry setup circuit. On a graph of impedance-velocity, the velocity corresponding to the point of infelation was reported the deposition velocity. The deposition velocities measured for sand–water mixture flows were compared with those calculated using previously reported empirical correlations where a deviation as small as 7.0% was found. In addition, it was proved that deposition velocities in biomass–water mixtures are well below common industrial pumping velocities, i.e., particle deposition is not an issue in biomass pipelines. The high-frequency impedancemetry approach was found to be a replacement for traditional techniques such as gamma ray densitometry, visual observations, and ERT systems, since it does not disturb/stop the slurry flow and is simple and economic to fabricate, easy to operate, easy to mount on the pipeline, applicable to all the suspensions conducting electricity, and capable of accurately measuring slurry deposition velocities as low as 0.04 m/s.

Acknowledgments

The authors are grateful to the National Sciences, Engineering Research Council of Canada (NSERC) for the financial support to carry out this project. As a part of the University of Alberta's Future Energy Systems research initiative, this research was made possible in part thanks to funding from the Canada First Research Excellence Fund. The authors are thankful to Astrid Blodgett for assistance with editing. However, all the results, justifications, and conclusion are solely the authors and have not been endorsed by any other party.

References

Abulnaga, B., 2002. Slurry Systems Handbook. McGraw-Hill, New York, NY.

Bott, L., 2006. Body composition in children with bronchopulmonary dysplasia predicted from bioelectric impedance and anthropometric variables: comparison with a reference dual X-ray absorptiometry. Clin. Nutr. 25, 810–815.

Brahimi, M., et al., 2010. The usefulness and limitations of combined fine-needle aspiration impedancemetry and flow cytometry in the diagnosis and subclassification of non-Hodgkin's lymphoma/leukemia (NHL). Hematol. J. 95, 614.

Caillette, A., et al., 1994. Total-body water determination using tetrapolar impedancemetry in capd patients. Nephrol. Dial. Transplant. 9, 585.

Coffey, G.R., Partridge, V.A., 1982. Coal slurry pipelines: the ETSI project. Right Way J. (August), 11–16.

Dezenclos, T., et al., 1994. Optimization of the indirect impedancemetry technique — a handy technique for microbial-growth measurement. Appl. Microbiol. Biotechnol. 42, 232–238.

Dheilly, A., et al., 2008. Monitoring of microbial adhesion and biofilm growth using electrochemical impedancemetry. Appl. Microbiol. Biotechnol. 79, 157–164.

Dickin, F., Wang, M., 1996. Electrical resistance tomography for process applications. Meas. Sci. Technol. 7, 247–260.

Durand, R., 1953. Basic relationships for the transportation of solids in pipes — experimental research. Minnesota International Hydraulics Convention, 89–103.

Durand, R., Condolios, E., 1952. The hydraulic transport of coal and solid material in pipes. In: Colloquium on Hydrotransport of Coal, National Coal Board London, UK.

Ellis, K.J., et al., 2000. Erratum: measurement of body water by multifrequency bioelectrical impedance spectroscopy in a multiethnic pediatric population. Am. J. Clin. Nutr. 71, 1618.

Fangary, Y.S., et al., 1998. Application of electrical resistance tomography to detect deposition in hydraulic conveying systems. Powder Technol. 95, 61–66.

Giguere, R., et al., 2008. Characterization of slurry flow regime transitions by ERT. Chem. Eng. Res. Des. 86, 989–996.

Gillies, R.G., et al., 2000. Deposition velocities for Newtonian slurries in turbulent flow. Can. J. Chem. Eng. 78, 704–708.

Gillies, R.G., Shook, C.A., 1991. A deposition velocity correlation for water slurries. Can. J. Chem. Eng. 69, 1225–1228.

Grzina, A., et al., 2009. Slurry Pump Handbook. Weir Slurry Group, Inc.

Lahiri, S.K., 2009. Study on Slurry Flow Modeling in Pipeline [dissertation]. Department of Chemical Engineering. National Institute of Technology, Durgapur.

Larsen, I., 1968. Hetrogeneous flow of solids in pipelines. J. Hydraul. Devision 94, 332.

Leitch, I., 2006. Handbook of Pumps and Pumping. Pumping Manual International, Newcastle, UK.

Mariano De Souza, J.C., et al., 2004. The Samarco pipeline — 26 years of operation. 16th Hydrotransport International Conference 2, 659–673.

Matousek, V., 2001. Distribution and friction of particles in pipeline flow of sand-water mixtures. In: Levy, A., Kalman, H. (Eds.), Handbook of Powder Technology. Elsevier Science, pp. 465–471.

Matousek, V., 2002. Pressure drops and flow patterns in sand-mixture pipes. Exp. Therm. Fluid Sci. 26, 693–702.

Nardi, J., 1959. Pumping Solids Through a Pipeline. Pipeline News, pp. 26–33.

Oroskar, A.R., Turian, R.M., 1980. The critical velocity in pipeline flow of slurries. AIChE J. 26, 550–558.

Sasic, M., Marjanovic, P., 1978. On the methods of calculation of hydraulic transportations and their reliability in practice. In: 5th International Conference on Hydraulic Transport of Solids in Pipes, Hanover, Germany, pp. 61–69.

Schlieper, G., 2000. Principles of gamma ray densitometry. Met. Powder Rep. 55, 20–23.

Shah, S.N., Lord, D.L., 1991. Critical velocity correlations for slurry transport with non-newtonian fluids. AIChE J. 37, 863–870.

Shook, C.A., 1969. Pipelining solids: the design of long-distance pipelines. In: Symposia in Pipeline Transport of Solids, The Canadian Society for Chemical Engineering Toronto, Canada.

Smye, S.W., et al., 1994. Total-body water determination using tetrapolar impedancemetry in capd patients. Nephrol. Dial. Transplant. 9, 585–586.

Turian, R.M., et al., 1987. Estimation of the critical velocity in pipeline flow of slurries. Powder Technol. 51, 35–47.

Vaezi, M., et al., 2014a. Investigation into the mechanisms of pipeline transport of slurries of wheat straw and corn stover to supply a bio-refinery. Biosyst. Eng. 118, 52–67.

Vaezi, M., 2014b. Experimental and Techno-economic Studies of Pipeline Hydro-transport of Agricultural Residue Biomass to a Biorefinery. Department of Mechanical Engineering University of Alberta, Edmonton.

Vaezi, M., Kumar, A., 2014. The flow of wheat straw suspensions in an open-impeller centrifugal pump. Biomass Bioenergy 69, 106–123.

Vaezi, M., et al., 2015. Is the pipeline hydro-transport of wheat straw and corn stover to a biorefinery realistic? Biofuels Bioprod. Biorefin. 9, 501–515.

Vaezi, M., et al., 2013. Lignocellulosic biomass particle shape and size distribution analysis using digital image processing for pipeline hydro-transportation. Biosyst. Eng. 114, 97–112.

Venton, P.B., 1982. Gladstone limestone pipeline. 8th Hydrotransport International Conference, 49–62.

Wasp, E.J., et al., 1977. Solid-liquid Flow in Slurry Pipeline Transportation. Trans-Tech Publications, Clausthal, Germany.

Weston, M.D., Worthen, L., 1987. Chevron phosphate slurry pipeline commissioning and start-up. In: 12th International Conference on Coal and Slurry Technology, Washington, DC.
Winter, C.H., et al., 2003. High temperature insulated coating aids construction of Alberta bitumen pipeline. Oil Gas J. 101, 56–58.
Yenjaichon, W., et al., 2011. Assessment of mixing quality for an industrial pulp mixer using electrical resistance tomography. Can. J. Chem. Eng. 89, 996–1004.
Zandi, I., Govatos, G., 1967. Hetrogenous flow of solids in pipes. J. Hydraul. Dev. 93, 145.